pp. 1–18 (2011)

Numerical issues of modelling blood flow in networks of vessels with pathologies

Yu. VASSILEVSKI*, S. SIMAKOV†, V. SALAMATOVA‡, Yu. IVANOV*, and T. DOBROSERDOVA§

Abstract — The synthesis of the blood circulation model and the elastic fiber model of the vessel wall allows us to take into account the influence of possible vessel pathologies on the global blood flow. The interaction is based on the state equation representing the dependence of the transmural pressure on the cross-section of the vessel. Numerical properties of both models are considered in the paper.

The mathematical modelling of blood circulation is a fundamental problem lying at the junction of several disciplines, such as differential equations, numerical analysis, elasticity theory, and physiology. Several numerical implementations of blood circulation models taking into account elastic properties of blood vessels were created in the last decade [6,9,10,14,21,22]. Previously we proposed an approach to synthesis of the blood circulation model and the elastic model of the vessel wall [24] taking into account the influence of possible vessel pathologies on the global blood flow. The distinctive feature of the approach is the use of merely one-dimensional differential operators, which provided us with an efficient numerical simulation technology. The mathematical blood flow model is a system of differential equations for each vessel linked by boundary conditions at the points of vessel junctions [22]. The mathematical model of the elastic vessel wall is based on the fiber approach [17,18] to the calculation of the reaction force as a response to the deformation of a fiber. The representation of an elastic body by sets of fibers of different configurations was successfully used for simulation of cardiac work [13] and collapsed veins [18]. In our model we used the same types of fibers as in [18].

The synthesis of both models is based on the state equation representing the dependence of the transmural pressure on the cross-section area of the vessel. This

*Institute of Numerical Mathematics, Russian Academy of Sciences, Moscow 119333, Russia
Corresponding author. E-mail: vasilevs@dodo.inm.ras.ru

†Moscow Institute of Physics and Technology, Dolgoprudny 141700, Russia

‡Scientific Educational Center of Institute of Numerical Mathematics RAS

§Lomonosov Moscow State University, Moscow 119991, Russia

The work was partly supported by the Federal Program ‘Academic and pedagogical staff of innovative Russia’, RAS program ‘Basic Research for Medicine’, joint French–Russian Programme International de Cooperation Scientifique (PICS) ‘Mathematical modelling of blood diseases’, by the Russian Foundation for Basic Research (09–01–00115, 10–01–91055, 11–01–00855).

dependence takes into account the elastic properties of the blood vessel and is a key characteristic of the vessel in the global blood circulation model. The state equation both for a healthy vessel and for the case of some pathology (an atherosclerotic plaque, an installed implant) can be calculated with the use of the fiber model of the blood vessel wall. Results of blood flow modelling in a system of healthy vessels and vessels with pathologies were presented in [7,22–25]. In this paper we consider numerical properties of the models of the global blood circulation and the vessel wall.

The paper is organized as follows. The second section presents the basic numerical methods used in our models. Numerical properties of the blood vessel wall model and peculiarities of solution methods are considered in the third section. The fourth section describes the global blood circulation model and discusses the peculiarities of its numerical implementation.

1. Numerical methods used in the models

1.1. Discretization of differential operators

The models considered in the paper (model of the elastic vessel wall and model of blood circulation) are based on a set of differential equations on one-dimensional curvilinear segments given in the three-dimensional space and interacting with each other. This formulation allows us to simplify the arising discrete systems as much as possible and to preserve simultaneously the flexibility and generality of the approach.

Consider the curvilinear segment $[x_0, x_N]$ and $N+1$ points $x_0, x_1, \ldots, x_N$ uniformly positioned on this segment and called the nodes of the calculation grid. Denote the midpoints of the segments $[x_i, x_{i+1}]$ by $x_{i+1/2}$ and a grid function defined at the nodes x_i by f_i. The finite difference discretization of the first-order differential operator is determined at the nodes $x_{i+1/2}$ in the usual way:

$$\frac{\mathrm{d}f}{\mathrm{d}s}(x_{i+1/2}) \approx \frac{f_{i+1} - f_i}{s_{i+1} - s_i} \tag{1.1}$$

where s_i is the distance along the segment from x_i to x_0. The discretization of the second-order operator at the nodes x_i is the successive application of two operations of finite difference differentiation (1.1). Under the assumption of a sufficient smoothness of the function f, both discretizations provide the second order of approximation with respect to the mesh size $\Delta s = s_1 - s_0 = \ldots = s_N - s_{N-1}$.

Note that, in addition to the differentiation of functions on a given segment, finite difference discretizations can be used for estimation of geometric characteristics of a curvilinear segment. For example, the curvature vector at the node x_i can be approximated by the formula

$$\frac{\mathrm{d}^2\mathbf{X}}{\mathrm{d}s^2}(x_i) \approx \frac{\boldsymbol{\tau}_{i+1/2} - \boldsymbol{\tau}_{i-1/2}}{\Delta s}, \qquad \boldsymbol{\tau}_{i+1/2} = \frac{\mathbf{X}_{i+1} - \mathbf{X}_i}{\Delta s} \tag{1.2}$$

where $\mathbf{X}$ is the coordinate vector of the node x in the three-dimensional space, $\boldsymbol{\tau}_{i+1/2}$ is the discretization of the tangent vector at the point $x_{i+1/2}$.

1.2. Solution of linear problems

The solution of the system of linear equations with a nondegenerate square matrix of coefficients

$$A\mathbf{x} = \mathbf{b} \tag{1.3}$$

is a well-developed numerical technology. In the case of dense matrices, the program package LAPACK [26] is the standard instrument for this purpose.

In the case of sparse matrices, iterative methods on Krylov subspaces are the most efficient. In the case of unsymmetric nondegenerate matrices, the commonly used methods are the generalized method of minimal residuals, GMRES, and the stabilized method of biconjugate gradients, BiCGStab [20]. In this paper we use the non-preconditioned BiCGStab method.

1.3. Solution of nonlinear systems

The basic solution method for systems of nonlinear equations of the form

$$\mathbf{F}(\mathbf{x}) = 0 \tag{1.4}$$

is the Newton method. In its canonical form, Newton's method assumes that the Jacobian $\mathbf{F}'(\mathbf{x})$ of the vector function $\mathbf{F}$ is known for any vector $\mathbf{x}$:

Algorithm 1.1.
Let $\mathbf{x}_0$ be given.
For $k = 0, 1, \ldots$ (until the convergence) do:
calculate the vector $\mathbf{s}_k$ from the linear system

$$\mathbf{F}'(\mathbf{x}_k)\mathbf{s}_k = -\mathbf{F}(\mathbf{x}_k) \tag{1.5}$$

assume

$$\mathbf{x}_{k+1} = \mathbf{x}_k + \mathbf{s}_k. \tag{1.6}$$

The convergence criteria can be different. For example, the Euclidean norm of the residual vector $\mathbf{F}(\mathbf{x}_k)$ must be less than the specified threshold. The convergence of Newton's method is quadratic and conditional on the closeness of the initial guess to the solution and on the assumption of the exact solution of linear systems (1.5). The local convergence of the method may cause difficulties in the solution of applied problems.

One of the modern solution technologies for nonlinear systems is the Inexact Newton Backtracking (INB) [1, 8, 16]. It does not require an exact solution of linear systems, nor the knowledge of a Jacobi matrix and combines the properties of global convergence with the properties of fast local convergence.

Algorithm 1.2.
Let $\mathbf{x}_0$, $\eta_{\max} \in [0,1)$, $t \in (0,1)$, and $0 < \theta_{\min} < \theta_{\max} < 1$ be given.
For $k = 0, 1, \ldots$ (until the convergence) do:
Assign initial $\eta_k \in [0, \eta_{\max}]$ to

$$\eta_k = \begin{cases} \min\{\eta_{\max}, \frac{|\|\mathbf{F}(\mathbf{x}_k)\| - \|\mathbf{F}(\mathbf{x}_{k-1}) + \mathbf{F}'(\mathbf{x}_{k-1})\mathbf{s}_{k-1}\|\|}{\|\mathbf{F}(\mathbf{x}_{k-1})\|}\}, & k > 0 \\ 0.5, & k = 0. \end{cases} \tag{1.7}$$

Calculate initial $\mathbf{s}_k$ so that

$$\|\mathbf{F}(\mathbf{x}_k) + \mathbf{F}'(\mathbf{x}_k)\mathbf{s}_k\| \leqslant \eta_k \|\mathbf{F}(\mathbf{x}_k)\|, \tag{1.8}$$

While $\|\mathbf{F}(\mathbf{x}_k + \mathbf{s}_k)\| > [1 - t(1-\eta_k)]\|\mathbf{F}(\mathbf{x}_k)\|$ do:

$$\begin{aligned} &\text{Take } \theta \in [\theta_{\min}, \theta_{\max}]; \\ &\text{Recalculate } \mathbf{s}_k \leftarrow \theta \mathbf{s}_k \text{ and } \eta_k \leftarrow 1 - \theta(1-\eta_k). \end{aligned} \tag{1.9}$$

Assign

$$\mathbf{x}_{k+1} = \mathbf{x}_k + \mathbf{s}_k. \tag{1.10}$$

The typical values of the parameters of this algorithm [16] are $\eta_{\max} = 0.9$, $\theta_{\min} = 0.1$, $\theta_{\max} = 0.5$, $t = 10^{-4}$. The algorithm has the theoretical justification [4,5] indicating its superlinear convergence and its global nature.

The iterative solution of (1.5) by a method on a Krylov subspace (e.g., BiCGstab) requires only the results of the multiplication of $\mathbf{F}'(\mathbf{x}_k)$ by a vector. This allows us to replace the action of the operator $\mathbf{F}'(\mathbf{x}_k)\mathbf{v}$ by its finite difference approximation. For example,

$$\mathbf{F}'(\mathbf{x}_k)\mathbf{v} = \frac{1}{\varepsilon}[\mathbf{F}(\mathbf{x}_k + \varepsilon\mathbf{v}) - \mathbf{F}(\mathbf{x}_k)]. \tag{1.11}$$

This variant of the Newton method is often called the Newton–Krylov method not using the Jacobian [8]. There exist several technical implementations of the algorithm [16, 27] admitting preconditioning of arising linear systems. In our calculations we use the implementation of [27] and do not apply any preconditioner. The arithmetical complexity of the method is expressed through the total number of evaluations of the function $n_{\mathrm{ev}F}$, the other costs may neglected.

2. Fiber models of the blood vessel wall

2.1. General fiber model and its application to healthy vessels and to vessels with pathologies

The elastic properties of blood vessel walls are mainly determined by a system of interweaved fibers (elastic, smooth muscle, collagenous) [2]. This peculiarity of the

histological structure of venous and arterial walls gives us the idea of simulating the elastic strain of a vessel by a set of fibers of different configurations, namely, by longitudinal, circular, and spiral fibers. The fiber approach used in this paper for the representation of an elastic shell was first proposed by Ch. Peskin and described in [17, 18].

Let $\mathbf{X} = \mathbf{X}(q,r,s,t)$ determine the motion equations for the material points of an incompressible elastic body in the chosen system of rectangular coordinates. Here $\mathbf{X} = (X_1, X_2, X_3)$ are the spatial coordinates of a moving point and q, r, s are the material coordinates individualizing the material point. Denote the elastic strain energy corresponding to some configuration of the solid body by $E[\mathbf{X}]$. As was shown in [17], one can conclude from the virtual work principle that the density of the force $\mathbf{f}$ of the elastic body reaction to the applied strain is equal to the Fréchet derivative of the strain energy

$$\mathbf{f} = -\frac{\delta E}{\delta \mathbf{X}} \tag{2.1}$$

where δ is the symbol of the variation.

Present here two essentially important cases. Let q, r, s be material curvilinear coordinates taken so that q, r are constant along each fiber. First consider the system of equally directed elastic fibers reacting only to stretch and subjected to a strain. The corresponding density of the force of elasticity has the form [13]:

$$\mathbf{f} = \frac{\partial}{\partial s}(T\boldsymbol{\tau}) \tag{2.2}$$

where T is the stress in the fiber, $\boldsymbol{\tau}$ is the unit tangent vector to the fiber

$$T = \sigma\left(\left|\frac{\partial \mathbf{X}}{\partial s}\right|\right), \qquad \boldsymbol{\tau} = \frac{\partial \mathbf{X}/\partial s}{|\partial \mathbf{X}/\partial s|}. \tag{2.3}$$

Consider another example. Let the system of elastic fibers be such that the fibers react only to bending and are subjected to a strain. Then the elastic strain energy and the corresponding elastic force density have the form [13]:

$$\mathbf{f} = \frac{\partial^2}{\partial s^2}\left(c_b(q,r,s)\frac{\partial^2 \mathbf{X}}{\partial s^2}\right) \tag{2.4}$$

where c_b is the coefficient characterizing the flexural rigidity of the fiber.

2.1.1. Healthy blood vessel. We assume that the blood vessel is a circular thin-wall cylindrical shell made of a linearly elastic material experiencing internal pressure [6]. The median surface of this shell is represented by some set of circular and longitudinal fibers. All these fibers resist only extension and compression and formulas (2.3), (2.2) are valid for them. The restriction posed by such type of fibers is

quite justified for this axisymmetric strain; however, for more complex load laws, naturally, it is necessary to model the shell by fibers of different types subject to bending, as well as tension and compression, which will be done in the near future. The use of the fiber model of an elastic wall allows us to take into account the nonlinear properties of blood vessel walls [2].

Let N_b be the number of computational nodes on the fiber, $\mathbf{X}_k$, $k = 1,\ldots,N_b$, characterizes the position of the kth point in the three-dimensional space, Δs is the distance between the adjacent points of the fiber in the unstrained state; then, according to formulas (2.2), (1.2), the discrete density of the elastic force is determined as

$$\mathbf{f}_k = \frac{T_{k+1/2}\boldsymbol{\tau}_{k+1/2} - T_{k-1/2}\boldsymbol{\tau}_{k-1/2}}{\Delta s}. \tag{2.5}$$

For a linearly elastic material with the Young modulus E, according to Hooke's law, we have

$$\sigma\left(\left|\frac{\partial \mathbf{X}}{\partial s}\right|\right) = E\left(\left|\frac{\partial \mathbf{X}}{\partial s}\right| - 1\right).$$

Let the points of intersection of circular and longitudinal fibers be the computational nodes on the fibers. Then the total discrete density of elastic forces $\mathbf{f}_{ij}$ at the nodes of the formed grid is the sum of the discrete densities of circular and rectilinear fibers. We assume that $\mathbf{f}_{ij}$ is constant over the surface area element S_{ij} and over the thickness of the vessel wall, i.e., the density of the elastic forces is a piecewise-constant function for the vessel wall. In the elementary volume of the vessel wall $S_{ij} \times h$, the elastic force $\mathbf{F}$ has the form

$$\mathbf{F} = \int_{S_{ij}\times h} \mathbf{f}_{ij}\mathrm{d}V = \mathbf{f}_{ij}S_{ij}h \tag{2.6}$$

where h is the thickness of the wall. This force countervails the pressure acting onto the inner vessel wall. Thus, the balance equation has the following form:

$$p = h\,\mathbf{f}_{ij}\cdot\mathbf{n}_{ij} \tag{2.7}$$

where $\mathbf{n}_{ij}$ is the normal to the corresponding element of the surface, p is the magnitude of the internal pressure. Relation (2.7) is basic for determining displacements of vessel points for the given internal pressure.

In order to check numerically the approximations of the shell model by the grid model of fiber representation, we take the following solution for the cylindrical shell made of a linearly elastic material under the internal pressure $P(z) = a_0 + a_1 z$ [11]:

$$\begin{aligned} u = u(z) &= \frac{P(z)R^2}{Eh}, \qquad v = 0 \\ w = w(z) &= -\frac{\nu R}{Eh}\left(a_0 z + a_1\frac{z^2}{2}\right) + \frac{\nu R}{Eh}\left(a_0 L + \frac{a_1 L^2}{2}\right) \end{aligned} \tag{2.8}$$

Table 1.
Relative error for the pressure function obtained by the fiber model for different parameters of the computational grid.

$N_z \times N_\theta$	$a_0 = 1$ kPa, $a_1 = 5$ kPa/cm	$a_0 = 0$ kPa, $a_1 = 5$ kPa/cm
16×128	8.5%	9.0%
32×128	4.7%	5.0%
64×128	2.5%	2.6%
128×128	1.2%	1.3%

where R, L, and h are the median radius, length, and shell thickness, respectively; u, v, w are the radial, circular, and axial displacements of shell points, respectively; E is the Young modulus, $\nu = 0.5$ is the Poisson coefficient, a_0 and a_1 are some numeric values which we can vary. Here and further, (r, θ, z) is the cylindrical system of coordinates.

Represent the shell of the vessel as N_z circular fibers discretized by the same number of points N_θ with the coordinates $\mathbf{X}_{ij} = (r_{ij}, \theta_{ij}, z_{ij})$, where $i = 1, \ldots, N_z$, $j = 1, \ldots, N_\theta$. Define the displacements of vessel points in accordance with formulas (2.8), i.e.,

$$\mathbf{X}^*_{ij} = \mathbf{X}_{ij} + u_{ij}\mathbf{e}_r + w_{ij}\mathbf{e}_z, \quad u_{ij} = u(z_{ij}), \quad w_{ij} = w(z_{ij}). \tag{2.9}$$

Using relation (2.5) for forces and balance equation (2.7), we calculate the values of the internal pressure p_{ij} at the nodes of the model of the strained vessel. In order to proceed from discrete values to the continuous function $P(\theta, z)^N$, we assume that

$$P(\theta, z)^N = p_{ij}, \quad \theta \in [\theta_{i,j-1/2}, \theta_{i,j+1/2}], \quad z \in [z_{i-1/2,j}, z_{i+1/2,j}]$$

where $\theta_{i,j+1/2}$ is the θ-component of the vector $\mathbf{X}_{i,j+1/2} = (\mathbf{X}_{i,j+1} - \mathbf{X}_{i,j})/2$ and $z_{i+1/2,j}$ is the z-component of the vector $\mathbf{X}_{i+1/2,j} = (\mathbf{X}_{i+1,j} - \mathbf{X}_{i,j})/2$. Then the L_2-norm of the difference between the analytic solution P and the numerical one $P(\theta, z)^N$ has the form

$$||P - P(\theta, z)^N||_{L_2} = \left(\sum_{i,j}^{N_z, N_\theta} \int_{\theta_{i,j-1/2}}^{\theta_{i,j+1/2}} \int_{z_{i-1/2,j}}^{z_{i+1/2,j}} (P(\theta, z) - p_{i,j})^2 \mathrm{d}\theta \mathrm{d}z \right)^{1/2}.$$

Due to the fact that the considered strain is axisymmetric, i.e., does not depend on θ, the number of computational nodes N_θ on the fiber does not influence numerical properties of the model. We study the approximative properties of the model depending on the number of fibers N_z. Table 1 presents the values of the L_2-norm of the error compared to the norm of the analytic function for the pressure. The grid fiber model provides the first-order convergence to the continuous solution of the problem for the shell model.

In the equilibrium problem of a blood vessel under internal pressure, the required displacements determine the form of the strained vessel. For axisymmetric

Table 2.
The number of evaluations of n_{evF} depending on different parameters of the computational grid and internal pressure.

$N_z \times N_\theta$	$a_0 = 6$ kPa $a_1 = 0$ kPa/cm	$a_0 = 0$ kPa $a_1 = 6$ kPa/cm	$a_0 = 6$ kPa $a_1 = 6$ kPa/cm
16×32	3	7	7
32×32	3	7	7
32×64	3	7	7
64×64	3	7	9
64×128	3	13	13
128×128	3	13	14
128×256	3	24	25
256×256	3	48	61

types of strain we can assume that displacement occurs in the radial direction only, then equilibrium condition (2.7) of the vessel under internal pressure has the form

$$\mathbf{f}(R+u(z)) \cdot \mathbf{n}(R+u(z))h - p = 0 \tag{2.10}$$

where R and h are the median radius and thickness of the shell, respectively, $u(z)$ is the radial displacement of shell points. Consider the case when the internal pressure has the form $p = a_0 + a_1 z$ and external pressure equals zero. Equation (2.10) is nonlinear with respect to the radial displacements of the points and is solved by INB solution methods for nonlinear equations described above in Section 1.3. The stop criterion for iterations is the following: the Euclidean norm of the residual vector is less than 10^{-6}. Table 2 presents the number of evaluations n_{evF} depending on the parameters a_0 and a_1, as well as N_z and N_θ, where N_z and N_θ is the number of circular fibers and the number of points in those fibers, respectively. The coefficients of the model are taken the same as in the previous case. The arithmetic complexity of the solution of the system depends on the computational grid and on the form of the function $p(z)$.

2.1.2. Atherosclerotic blood vessel. In spite of the existence of different viewpoints relative to the pathogenesis of atherosclerosis [15, 19], the following conception of atherosclerotic formation is commonly accepted. According to this conception, a lipid core is formed in the vessel wall and is separated from the lumen of the vessel by a fibrous cap.

Thus, we consider an atherosclerotic vessel as a three-layered cylindrical shell under internal pressure. The inner and outer layers of the shell are the fibrous cap and the artery wall, respectively. The strain of the fibrous cap and the vessel wall are modelled with the help of the fiber representation described above.

In order to calculate the strains and elastic forces arising in the lipid core under pressure from the pulsating blood flow, it is assumed that its response is equivalent to the response of a set of 'springs' uniformly distributed over its length. We assume that the influence of tangent stresses is small and the oscillations of such 'strings'

are possible in the radial direction only. For the physiologically admissible range of internal and external pressures, the determination of 'springs' stiffness can be performed by solving analytically the problem of an isotropic elastic cylinder ($a \leqslant r \leqslant b$) under the external p_b and internal p_a pressures in the context of the linear theory of elasticity. This solution has the form

$$p_a - p_b = \frac{2(b^2 - a^2)E_c r}{3a^2 b^2} u(r) \tag{2.11}$$

where E_c is the modulus of elasticity of the cylinder, $u(r)$ is the radial displacement of the cylinder points.

Let $a \leqslant r \leqslant b$ determine the middle lipid layer of the three-layered shell. By $u^a(\theta, z)$ and $u^b(\theta, z)$ we denote the displacements of the points of the fibrous cap and artery wall, respectively; p_a and p_b are the magnitudes of the contact pressure on the boundaries $r = a$ and $r = b$, respectively. Then, according to formula (2.7), the equilibrium conditions for the outer (vessel wall) and inner (fibrous cap) layers can be represented in the form

$$p_a = p_0 - h^{\text{cap}} \mathbf{f}^{\text{cap}} \cdot \mathbf{n}^{\text{cap}} \tag{2.12}$$

$$p_b = h^{\text{art}} \mathbf{f}^{\text{art}} \cdot \mathbf{n}^{\text{art}} \tag{2.13}$$

where $\mathbf{f}^{\text{art}} = \mathbf{f}(b + u^b(\theta, z), \theta, z)$, $\mathbf{n}^{\text{art}} = \mathbf{n}^{\text{art}}(b + u^b(\theta, z), \theta, z)$, h^{art} and $\mathbf{f}^{\text{cap}} = \mathbf{f}(a + u^a(\theta, z), \theta, z$, $\mathbf{n}^{\text{cap}} = \mathbf{n}^{\text{cap}}(a + u^a(\theta, z), \theta, z$, h^{cap} are the elastic force, normal to the surface, layer thickness of the artery wall and fibrous cap, respectively; $\mathbf{f}$ is the density of the elastic force determined by formula (2.2); p_0 is the value of the internal pressure.

According to (2.11)–(2.13), for $r = a$ and $r = b$ we can get a system of nonlinear equations for $u^a(\theta, z)$ and $u^b(\theta, z)$.

In order to compose a numerical model for an atherosclerotic vessel, we represent the three-layered shell with the help of N_z pairs of concentric circular fibers linked by radial 'springs' described above. Concentric fibers are uniformly distributed along the length of the vessel and lie in the corresponding section $z = z_i$, $i = 1, \ldots, N_z$. Let each circular fiber be discretized by the same number of points uniformly distributed over the fiber with the angular coordinate θ_k, $k = 1, \ldots, N_\theta$. Then with respect to $u^a(\theta, z)$, $u^b(\theta, z)$ the discretized system has the form

$$\begin{cases} h_{ik}^{\text{art}} \mathbf{f}_{ik}^{\text{art}} \cdot \mathbf{n}_{ik}^{\text{art}} + h_{ik}^{\text{cap}} \mathbf{f}_{ik}^{\text{cap}} \cdot \mathbf{n}_{ik}^{\text{cap}} - u_{ik}^a 2(b^2 - a^2)E_c a/(3ab^2) - p_0 = 0 \\ h_{ik}^{\text{art}} \mathbf{f}_{ik}^{\text{art}} \cdot \mathbf{n}_{ik}^{\text{art}} + h_{ik}^{\text{cap}} \mathbf{f}_{ik}^{\text{cap}} \cdot \mathbf{n}_{ik}^{\text{cap}} - u_{ik}^b 2(b^2 - a^2)E_c b/(3a^2 b) - p_0 = 0 \end{cases} \tag{2.14}$$

where

$$\mathbf{f}_{ik}^{\text{cap}} = \mathbf{f}(a + u_{ik}^a, \theta_k, z_i), \quad \mathbf{f}_{ik}^{\text{art}} = \mathbf{f}(b + u_{ik}^b, \theta_k, z_i)$$

$$\mathbf{n}_{ik}^{\text{cap}} = \mathbf{n}(a + u_{ik}^a, \theta_k, z_i), \quad \mathbf{n}_{ik}^{\text{art}} = \mathbf{n}(b + u_{ik}^b, \theta_k, z_i).$$

Table 3.
The number of evaluations n_{evF} for different parameters of the computational grid and the vessel lumen blocking.

$N_z \times N_\theta$	50%	70%	90%
16×32	23	21	21
32×32	23	21	22
32×64	43	41	42
64×64	43	41	42
64×128	77	79	86
128×128	79	81	86

System (2.14) contains $2N_zN_\theta$ nonlinear equations with respect to $2N_zN_\theta$ unknowns u^a_{ik}, u^b_{ik} and is solved by the INB method described in Algorithm 1.2. Table 3 presents the number of evaluations n_{evF} (the vector function F of system (2.14)) depending on N_z, N_θ with different values of the vessel lumen blocking. The coefficients of the model are $E_c = 1$ kPa, $p_0 = 10$ kPa, $a = 0.45$ cm, $b = a\sqrt{1-pr}$ cm, $h^{\rm cap} = h^{\rm art} = 0.07$ cm, $pr = 0.5, 0.7, 0.9$ is the rate of the vessel lumen blocking. The arithmetic complexity of the solution of equilibrium system (2.14) is proportional to N_θ and actually does not depend on N_z.

The approach described above can be applied to the calculation of state equation, i.e., determination of the dependence of transmural pressure on the cross-section area. In this case we can consider either a healthy vessel, or a vessel with different pathologies or implants whose influence can be simulated by additional functions of the internal pressure.

2.2. Reconstruction of the coefficients of the fiber model

In order to get an adequate description of the elastic strain in a blood vessel, it is necessary to define the stiffness constant of the fibers correctly. In this section we demonstrate the technique of determination of the unknown model parameters from its input data; those unknowns are the state equations for various types of vessels obtained from experiments. The solution to this problem makes it possible to calibrate the model of the elastic vessel wall for a particular patient and also for the case of various vascular pathologies. The degree of concordance of the parameters obtained from fiber representations means here the closeness in the L_2-norm of the state equation reconstructed by the model and the continuous piecewise-linear function interpolating the experimental data.

The adjustment of the fiber stiffness constant is performed using the known state equation by the following hierarchical algorithm. Let E_k, $k = 1, \ldots, N$, be the unknown model parameters, for each parameter the range of admissible values $D^0_k = [a^0_k, b^0_k]$ and the number q of divisions of the intervals D^0_k are given. We assume that $\{E^j_k = a^0_k + j|b^0_k - a^0_k|/q,\ j = 0, \ldots, q\}$, determine the set of all possible values for each E_k. Take a set $\{E^{s_1}_1, \ldots, E^{s_N}_N\}$ from all possible sets of parameters $\{E^{j_1}_1, \ldots, E^{j_N}_N\}$, $j_1, \ldots, j_N = 1, \ldots, q$, so that the target function (in our case this is

the state equation) calculated on this set deviates minimally from the given state equation. Taking into account the obtained set of parameters, we refine the domain of possible values, namely, at the next step for each E_k, $k = 1,\dots,N$, we take the interval $D_k^1 = [E_k^{s_k} - (b_0^k - a_0^k)/(2q),\ E_k^{s_k} + (b_0^k - a_0^k)/(2q)]$ as the new range of variation of E_k. The whole procedure is iterated as described above until we get the required accuracy.

Thus, the optimal parameter E_k^* is obtained in the interval D_k^0 with the accuracy $\delta_k = |D_k^0|/q^W$ in W steps of the algorithm. Note that the complexity of the algorithm grows as an exponential function of the number N of parameters, which restricts its efficient use to problems with a small number of parameters.

Let us apply the approach described here for the determination of the fiber stiffness in the case of an atherosclerotic vessel (Section 2.1.2) and for the fiber model of a vein. In both cases we assumed that the state equation $p = p(S)$ was given by some analytic function.

We take the solution of the linear elasticity problem for a three-layered cylinder loaded by internal pressure as the known state equation for an atherosclerotic vessel. Each layer is one particular component of the diseased vessel, namely, the fibrous cap, the lipid core, or the artery wall, and is characterized by the corresponding modulus of elasticity. The state equation has the following form in this case:

$$\begin{aligned} p &= C(\sqrt{S} - r_f) \\ C &= \frac{(r_a + h_a)^2(r_a^2(r_l^2 - r_f^2)E_f + r_f^2(r_a^2 - r_l^2)E_l) + r_f^2 r_l^2 h_a(2r_a + h_a)E_a}{2(r_a + h_a)r_a^2 r_l^2 r_f} \end{aligned} \tag{2.15}$$

where $E_f, E_a, E_l, r_f, r_l, r_a$ are the Young moduli and inner radii of the fibrous cap, the lipid core, or the artery wall, respectively; h_a is the thickness of the artery wall.

In order to solve the inverse problem, we take the Young moduli for the circular fibers responsible for the behaviour of the fibrous cap of the plaque and the artery wall as two unknowns of the model. The stiffness of the lipid layer is supposed to be known (1 kPa), because the variation of this parameter within a reasonable range produces no essential influence on the state equation reconstructed by this model.

The algorithm determining the unknown fiber stiffnesses was tested on some sets $\{E_f^{(i)}, E_a^{(i)}\}$ of Young moduli of the fibrous cap and the artery wall. As was said above, according to [3], we always assumed $E_a = 1$ kPa. The thickness of the artery wall was $h_a = 0.07$ cm. The range of both unknown elasticity moduli ranges from 1 kPa to 200 kPa, the number of partitions is $q = 4$, the number of steps is $W = 4$. Figure 1a shows the graph of the reconstructed state equation of the model for an atherosclerotic vessel (red line) and the input data (green marker), where S_0 is the cross-section area of the healthy artery under zero transmural pressure for the first set $E_a^{(1)} = 100$ kPa, $E_f^{(1)} = 100$ kPa. For other sets of constants ($E_a^{(2)} = 100$ kPa, $E_f^{(2)} = 50$ kPa; $E_a^{(3)} = 100$ kPa, $E_f^{(3)} = 10$ kPa; $E_a^{(4)} = 10$ kPa, $E_f^{(4)} = 100$ kPa) the graphs of the reconstructed equations have a form similar to that of Fig. 1a. In all cases the error of the reconstructed equation does not exceed 2%.

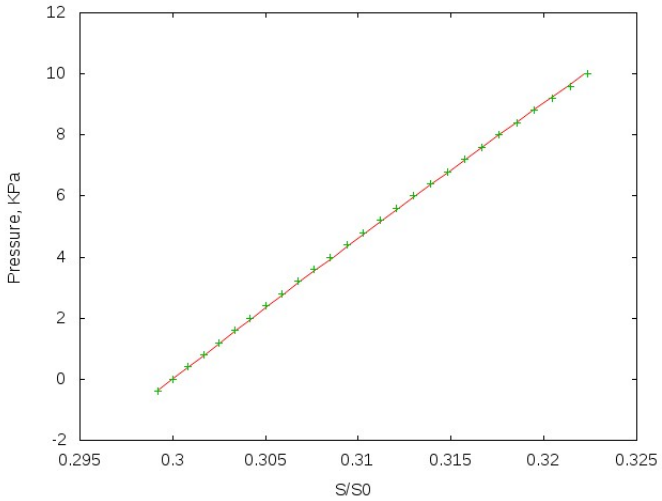

(a)

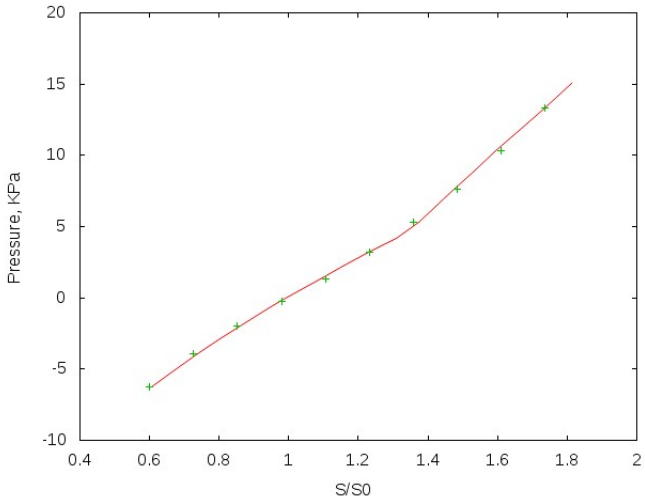

(b)

Figure 1. Reconstructed state equation of the model for (a) atherosclerotic vessel (solid line) and input data (cross marker) for $E_a^{(1)} = 100$ kPa, $E_f^{(1)} = 100$ kPa), (b) venous wall (solid line) and input data (cross marker)

Due to the hemodynamic peculiarities of a vein [2], we introduced a special set of fibers with the additional parameter R_c characterizing the rate of response delay to a fiber strain; in the case of a linear material it is taken into account according to

the formulas

$$\sigma\left(\left|\frac{\partial \mathbf{X}}{\partial s}\right|\right) = E_c\left(\left|\frac{\partial \mathbf{X}}{\partial s}\right| - R_c\right), \quad \left|\frac{\partial \mathbf{X}}{\partial s}\right| > R_c \tag{2.16}$$

$$\sigma\left(\left|\frac{\partial \mathbf{X}}{\partial s}\right|\right) = 0, \ \left|\frac{\partial \mathbf{X}}{\partial s}\right| \leqslant R_c. \tag{2.17}$$

The solution of the inverse problem for the venous wall is reduced to the determination of the following three parameters: E_e is the Young modulus of the set of circular fibers responsible for the behaviour of elastic and smooth muscle fibers, E_c and R_c are the Young modulus and the delay rate for the set of circular fibers simulating the behaviour of the collagen. Figure 1b shows the reconstructed state equation of the model obtained from the solution of the inverse problem where the nonlinear form of the vein state equation reflects the behaviour under negative transmural pressures and S_0 is the vein cross-section area before deformation under zero transmural pressure. The error of the reconstructed state equation does not exceed 2% in this case. It is worth noting that under the decreasing transmural pressure the form of the initially circular cross-section now becomes elliptic, and for negative values of the transmural pressure the cross-section has a dumb-bell form, i.e., it corresponds to two almost circular small channels separated by a flattened part of the vein [2].

3. Closed model of blood circulation

3.1. Assumptions and equations of the model

In this paper we consider the global blood circulation model [22] including the description of the blood flow in a network of elastic pipes simulating arteries and veins of systemic and pulmonary circulations. This network model is closed by a dynamic model of a four-chamber heart. The blood is assumed to be a viscous incompressible fluid flowing via the network of elastic pipes due to the pulse generated by the compression of the heart ventricle.

It is supposed that for most blood vessels the ratio of their diameter to their length is sufficiently small and hence the mathematical description is constructed in terms of the linear blood flow velocity and pressure averaged over cross-sections. Then the mass and momentum balance equations can be written for each vessel in the form

$$\frac{\partial S}{\partial t} + \frac{\partial (Su)}{\partial x} = 0 \tag{3.1}$$

$$\frac{\partial u}{\partial t} + \frac{\partial\left(\frac{u^2}{2} + \frac{p}{\rho}\right)}{\partial x} = -16\mu u \eta\left(\hat{S}\right) \tag{3.2}$$

where t is the time, x is the coordinate along the vessel, ρ is the blood density, $S(t,x)$ is the vessel cross-section area, $u(t,x)$ is the linear blood flow velocity averaged

over the cross-section, p is the pressure (relative to the atmospheric one), $\hat{S} = S/\bar{S}$, $\bar{S}$ is the cross-section area of the vessel for zero blood flow and zero transmural pressure $p(S) - p_*$, p_* is the pressure in the tissues surrounding the vessel; μ is the coefficient of friction;

$$\eta\left(\hat{S}\right) = \begin{cases} 2\hat{S}^{-1}, & \hat{S} \geqslant 1 \\ 1 + \hat{S}^{-2}, & \hat{S} < 1. \end{cases} \tag{3.3}$$

The elastic properties of vessel walls are given by the state equation. This equation may have the analytic form

$$p(S) - p_* = \rho c_0^2 f(S) \tag{3.4}$$

where c_0 is the spread velocity of small perturbations in the vessel wall, or may be determined by solution of static equilibrium problem for the vessel wall (see Section 2).

It is proposed to define the boundary conditions at the points of junction of the vessels with each other (anastomosis, vein junction) as the set of conditions formed by Poiseuille pressure drop conditions, the mass balance, and the compatibility condition for system (3.1)–(3.4):

$$p_k\left(S_k\left(t,\tilde{x}_k\right)\right) - p^l_{\text{node}}(t) = \varepsilon_k R^l_k S_k\left(t,\tilde{x}_k\right) u_k\left(t,\tilde{x}_k\right), \quad k = k_1, k_2, \ldots, k_M \tag{3.5}$$

$$\sum_{k=k_1,k_2,\ldots,k_M} \varepsilon_k S_k\left(t,\tilde{x}_k\right) u_k\left(t,\tilde{x}_k\right) = 0 \tag{3.6}$$

where l is the number of the junction domain (node), k is the number of the vessel, $k_1, k_2, \ldots, k_M$, M is the number of vessels meeting at the node, $p^l_{\text{node}}(t)$ is the pressure at the node, R^l_k is the hydraulic resistance for the flow from the vessel with the number k into the vessel with the number l. For the vessels outgoing from the node we have $\varepsilon_k = 1$, $\tilde{x}_k = L_k$, for the vessels incoming to the node we have $\varepsilon_k = -1$, $\tilde{x}_k = 0$. In the domains of the junction with the heart the product $S_k(t,x)\, u_k(t,x)$ is replaced in (3.5), (3.6) by the value of the voluminal blood flow to/from the corresponding chamber Q_k. A more detailed description of the dynamic four-chamber heart model used here can be found, e.g., in [22].

3.2. Numerical properties of the model

In the construction of an efficient numerical implementation of problem (3.1), (3.6) of the blood flow in a vascular network, one should take into account a large number of structural elements (vessels) and also the essential geometrical distinctions between those elements (lengths, diameters, elastic properties).

In order to calculate the blood flow in a single vessel, formulas (3.1), (3.6), the model uses several different schemes including first-order monotone schemes and a hybrid scheme corresponding to the most accurate first-order monotone scheme and the less oscillating scheme of the second order of accuracy [12]. The use of explicit

methods causes the necessity to analyze the stability of the scheme and to choose the corresponding time step

$$\tau_{n+1} = 0.9 s_{\max} \tag{3.7}$$

where $s_{\max} = \max_{k,i} |\lambda_{ki}|/h_k$, k belongs to the set of the indices of all the vessels of the considered network, i belongs to the set of all inner point indices of the finite difference grid of the vessel k, λ_{ki} is the eigenvalue of the Jacobian of system (3.1)-(3.4) maximal in its absolute value at the given points of the considered vessel (see details in [22]).

From the viewpoint of a numerical implementation of this model, the most critical block is the module calculating the points of the vessel junctions. In the domains of vessel junction we have to solve the nonlinear system of algebraic equations obtained after the discretization of boundary conditions (3.5), (3.6) and the compatibility condition for (3.1)–(3.4) along the characteristic leaving the integration domain for problem (3.1), (3.6). It should be taken into account that the vessels with essentially different parameters (lengths, diameters, elastic properties, spatial mesh sizes) and different flow modes (blood flow velocity and pressure) can be joined at one point. This essentially complicates the choice of the method convergent for all sets of parameters from the physiologically reasonable range. An equivalent system, whose dimension is half as much was obtained by identical transformations; this system can be solved by Newton's method (Algorithm 1.1) with the necessary restrictions

$$\mathbf{F}(\mathbf{S}) = \Delta\mathbf{f} + \mathbf{R}\mathbf{P} = \mathbf{0}. \tag{3.8}$$

Here

$$\mathbf{f} = \{\varepsilon_{k_m}(\alpha_{k_m} S_{k_m} + \beta_{k_m}) S_{k_m}\}_{m=1}^{M}, \quad \mathbf{P} = \{p_{k_m}\}_{m=1}^{M} \tag{3.9}$$

$$\mathbf{R} = \{R_{ij}\}_{i,j=1}^{M}, \quad R_{ii} = -\sum_{\substack{j=1 \\ j\neq i}}^{M} \prod_{\substack{m=1 \\ m\neq i \\ m\neq j}}^{M} R_{k_m}^{l}, \quad R_{ij} = \prod_{\substack{m=1 \\ m\neq i \\ m\neq j}}^{M} R_{k_m}^{l}, \quad \Delta = \det\mathbf{R} = \sum_{i=1}^{M} \prod_{\substack{j=1 \\ j\neq i}}^{M} R_{k_j}^{l} \tag{3.10}$$

where $\mathbf{R}$ is the symmetric matrix determining the hydraulic resistance for flows between the vessels joined at one node, α_{k_m} and β_{k_m} are the coefficients obtained after the discretization of the compatibility condition for system (3.1)–(3.4) at the current time step, M is the number of vessels joined at one node, k_m is the index of the mth vessel. The values from the previous time step are used as the initial guess for the iterative process. Numerical experiments showed that this choice of the initial guess satisfies all necessary restrictions and provides a fast convergence of the method.

Numerical experiments were performed for a vascular system represented by two connected networks of arteries and veins (341 vessels and 335 points of branching). There were 162 points of connection of the veins and arteries. The system described above was solved by Newton's method at each point. We considered nodes

differing in the number of incoming/outgoing vessels, their properties, and the blood flow intensity; these were points of junction of three vessels with identical or similar diameters (for example, 0.7 cm), but with different peak blood velocities (1–2 cm/s, 30–40 cm/s, 80–90 cm/s), points of junction of three vessels of different diameters (for example, 1.8, 1.7, and 1 cm), points of junction of four vessels of different diameters (for example, 1.4, 1.4, 0.7, and 0.7 cm). We also studied points of junction of veins and arteries, i.e., vessels with different elastic properties (c_0=700 cm/s and c_0=350 cm/s for the analytic form of state equation (3.4)). The elastic properties of the vessel wall were described both with the help of the analytic approximation [22], and with the help of fiber and spring-fiber models representing the response of the wall either for a healthy vessel, or in the presence of atherosclerotic plaques of different types, or in the presence of the cava filter [23–25]. In all the cases indicated here, Newton's method converged in 2–4 iterations for the given accuracy 10^{-6}, and in 3–4 iterations for the accuracy from 10^{-8} to 10^{-12}. The velocity in the joined vessels has the most essential influence on the number of iterations necessary for attaining the required accuracy. A greater number of iterations is required for the pulse wave maximum passing through the node. This is explained by the decrease in the initial guess accuracy due to the increase in the gradients of the calculated values. The application of this approach is restricted by the magnitude of the maximal admissible flow through a node. The numerical experiments performed here showed that this maximum lies beyond the range of physiologically reasonable values.

In numerical simulation of the heart blood flow, the main factor influencing the choice of the method is the stiffness of the system of differential equations [22] caused by the parameters from the physiologically reasonable range. The system was solved by the implicit one-step A- and L-stable method of the third order approximation from the family of continued schemes.

The advantage of the approach to construction of the numerical implementation described here is the ability to split problems into independent blocks for the calculation of the flow in each vessel and at each point of their junction.

4. Conclusion

The mathematical models of the blood flow and the blood vessel wall are described and their numerical properties are studied. It is proposed to simulate a vessel by the fiber approach proposed by Ch. Peskin. The first-order approximation of the fiber representation of the blood vessel wall has been obtained in experiments. The numerical determination of the state equation is based on the solution of the problem on the form of a vessel under internal pressure. The system of nonlinear equations appearing here is solved by the inaccurate Newton method where the number of evaluations of the nonlinear function grows moderately with the growth of the number of grid nodes. The solution of inverse problems is discussed in the paper, these problems allow us to determine unknown constants for each set of elastic fibers and to adjust the fiber model to a particular patient. The iterative algorithm for determination of the fiber stiffness is proposed, its error appears to be less than 2% in examples of an atherosclerotic vessel and a vein.

In the numerical implementation of the hemodynamic model, the greatest challenge is the calculation of vessel junction points. The system of nonlinear equations at a nodal point is reduced to the form little sensitive to the values of functional and geometric parameters of the linked vessels. The number of iterations required for attaining the accuracy 10^{-12} is less than 4 for all observed sets of the parameters from the physiologically reasonable range of values.

The models discussed here were used in [7, 23–25], where the problems of blood circulation were studied for a vein with an installed cava filter and for vessels with axisymmetric atherosclerotic plaques. In what follows, we plan to add into the model of the vessel wall the families of fibers of different configurations, which can resist compression and tension, as well as bending according to the nonlinear laws typical for biological tissues.

References

1. P. Brown and Y. Saad, Hybrid Krylov methods for nonlinear systems of equations. *SIAM J. Sci. Statist. Comput.* (1990) **11**, 450–481.
2. C. G. Caro, T. J. Pedley, R. C. Schroter, and W. A. Seed, *The Mechanics of the Circulation*. Oxford University Press, New York, 1978.
3. G. Cheng, H. Loree, R. Kamm, M. Fishbein, and R. Lee, Distribution of circumferential stress in ruptured and stable atherosclerotic lesions: a structural analysis with histopathological correlation. *Circulation* (1993) **87**, 1179–1187.
4. S. Eisenstat and H. Walker, Globally convergent inexact Newton methods. *SIAM J. Optim.* (1994) **4**, 393–422.
5. S. Eisenstat and H. Walker, Choosing the forcing terms in an inexact Newton method. *SIAM J. Sci. Comput.* (1996) **17**, 16–32.
6. L. Formaggia, A. Quarteroni, and A. Veneziani, *Cardiovascular Mathematics.* Vol. 1. Springer, Heidelberg, 2009.
7. Yu. Ivanov and T. Dobroserdova, Mathematical modelling of cava filter installation on the hemodynamics of blood vascular system. *Nauchn. Tekhn. Vestnik St. Petersburg Nat. Res. Univ. Inform. Technol. Mech. Optics* (2010) **68** No. 4, 94–98.
8. C. Kelley, *Iterative Methods for Linear and Nonlinear Equations*. SIAM, Philadelphia, 1995.
9. V. Koshelev, S. Mukhin, T. Sokolova, N. Sosnin, and A. Favorskii, Mathematical modelling of cardiovascular system hemodynamics subject to neuroregulation. *Math. Model.* (2007) **19**, No. 3, 15–28.
10. V. Koshelev, S. Mukhin, N. Sosnin, and A. Favorskii, *Mathematical Models of Quasi-One-Dimensional Hemodynamics*. MAKS Press, Moscow, 2010 (in Russian).
11. A. E. H. Love, *A Treatise on the Mathematical Theory of Elasticity*. Dover Publications, New York, 1934.
12. K. Magomedov and A. Kholodov, *Grid-Characteristic Numerical Methods*. Nauka, Moscow, 1988 (in Russian).
13. D. McQueen and C. Peskin, Heart simulation by an immersed boundary method with formal second-order accuracy and reduced numerical viscosity. In: *Mechanics for a New Millennium, Proc. Int. Conf. Theor. and Appl. Mech. (ICTAM) 2000* (Eds. H. Aref and J. W. Phillips). Kluwer Acad. Publ., 2001.

14. J. P. Mynard and P. Nithiarasu, A 1D arterial blood flow model incorporating ventricular pressure, aortic valve and regional coronary flow using the locally conservative Galerkin (LCG) method. *Commun. Numer. Meth. Engrg.* (2008) **24**, No. 5, 367–417.

15. Yu. Nesterov, *Atherosclerosis: Diagnostics, Treatment, Prevention*. Phoenix Publ., Rostov-on-Don, 2007 (in Russian).

16. M. Pernice and H. Walker, NITSOL: a Newton iterative solver for nonlinear systems. *SIAM J. Sci. Comput.* (1998) **19**, 302–318.

17. C. Peskin, The immersed boundary method. *Acta Numerica* (2002) **11**, 479–517.

18. M. Rosar and C. Peskin, Fluid flow in collapsible elastic tubes: a three-dimensional numerical model. *New York J. Math.* (2001) **7**, 281–302.

19. R. Ross, Atherosclerosis — An inflammatory disease. *New Engl. J. Med.* (1999) **2**, 115–126.

20. Y. Saad. *Iterative Methods for Sparse Linear Systems*. SIAM, Philadelphia, 2003.

21. S. J. Sherwin, V. Franke, J. Peiro, and K. Parker, One-dimensional modelling of vascular network in space-time variables. *J. Eng. Math.* (2003) **47**, 217–250.

22. S. Simakov and A. Kholodov, Computational study of oxygen concentration in human blood under low frequency disturbances. *Math. Mod. Comp. Sim.* (2009) **1**, 283–295.

23. Yu. Vassilevski, S. Simakov, and S. Kapranov, A multi-model approach to intravenous filter optimization. *Int. J. Numer. Meth. Biomed. Engrg.* (2010) **26**, 915–925.

24. Yu. Vassilevski, S. Simakov, V. Salamatova, Yu. Ivanov, and T. Dobroserdova, Blood flow simulation in atherosclerotic vascular network using fiber-spring representation of diseased wall. *Math. Model. Nat. Phenom.* (2011) **6**, No. 5, 333–349.

25. Yu. Vassilevski, S. Simakov, V. Salamatova, Yu. Ivanov, and T. Dobroserdova, Vessel wall models for simulation of atherosclerotic vascular networks. *Math. Model. Nat. Phenom.* (2011) **6**, No. 7, 82–99.

26. http://www.netlib.org/lapack/

27. http://www.sourceforge.org/projects/ani2d/